Resonant acoustic transmission through compound subwavelength hole arrays: the role of phase resonances

2009 J. Phys.: Condens. Matter 21 445401

(http://iopscience.iop.org/0953-8984/21/44/445401)

IOP PUBLISHING JOURNAL OF PHYSICS: CONDENSED MATTER

J. Phys.: Condens. Matter **21** (2009) 445401 (5pp) doi:10.1088/0953-8984/21/44/445401

Resonant acoustic transmission through compound subwavelength hole arrays: the role of phase resonances

Zhifeng Liu and Guojun Jin[1]

National Laboratory of Solid State Microstructures and Department of Physics, Nanjing University, Nanjing 210093, People's Republic of China

E-mail: gjin@nju.edu.cn

Received 12 July 2009, in final form 1 September 2009
Published 15 October 2009
Online at stacks.iop.org/JPhysCM/21/445401

Abstract

We study the resonant acoustic transmission through compound subwavelength periodic hole arrays. Fabry–Perot resonance peak splitting is found. We can attribute the phenomenon to phase resonances via calculating the phase difference between adjacent holes in a unit cell. Furthermore, by analyzing the transmission characteristics of different kinds of compound hole arrays for normal and non-normal incidence, it can be demonstrated that the phase resonances arise from the coupling between holes in a unit cell. In addition, we also discuss the transmission resonance originating from acoustic surface modes and illustrate the hybridized features of acoustic surface modes and Fabry–Perot modes. The results are expected to have advantages in tailoring resonant acoustic transmission properties.

(Some figures in this article are in colour only in the electronic version)

Extraordinary optical transmission (EOT) through the arrays of subwavelength holes in metallic films has attracted much attention since the pioneering work of Ebbesen *et al* [1]. Two main mechanisms leading to the EOT have been established: surface plasmon resonances [2–6] and localized waveguide resonances [7–9]. Recently, the idea of EOT has been transferred to the acoustic case and, like for light, extraordinary acoustic transmission (EAT) has been confirmed for plates with one-dimensional periodic arrays of grooves [10] or slits [11, 12] and two-dimensional periodic arrays of holes [13–15]. Unlike the physical origin of EOT, that of EAT has been mainly attributed as the excitation of acoustic surface waves (ASWs) [10] arising from the surface periodicity and the Fabry–Perot (FP) resonances [13–15] in individual holes and the hybridization between them [14]. On the other hand, for the electromagnetic case the so-called phase resonances, appearing in the transmittance as sharp dips, have been reported in one-dimensional compound metallic gratings [16–20]. Like for the electromagnetic counterpart, it is also expected that phase resonances will occur in the acoustic transmission through compound subwavelength hole arrays.

[1] Author to whom any correspondence should be addressed.

In this paper, we present a theoretical study of the acoustic transmission through compound subwavelength periodic hole arrays. We show the sharp dips, leading to the splitting of FP resonance peaks, appear in the transmittance when extra holes are added per unit cell. By investigating the field phases in different holes in a unit cell, we can conclude that the appearance of transmission dips arises from the field–phase interference between holes, i.e. when the phase difference between holes approaches π, their interference can induce a phase resonance dip. Next, by discussing the transmission resonance resulting from ASWs, the hybridized features, of acoustic surface modes and FP modes, are further demonstrated.

In figure 1, we schematically show four subwavelength hole unit cells perforated on brass plates with the thickness $h = 2$ mm and these unit cells can be used to form the compound periodic hole arrays. Figure 1(a) represents a simple periodic hole array, a unit cell consisting of only one square hole. We chose the hole size 1.063 mm $\times$ 1.063 mm and the period $d = 2$ mm, which present the same hole filling fraction 0.282 and array period 2 mm as the array of circular holes studied in [13]. Figures 1(b)–(d) show compound hole arrays with the identical array period $d = 2$ mm and hole filling

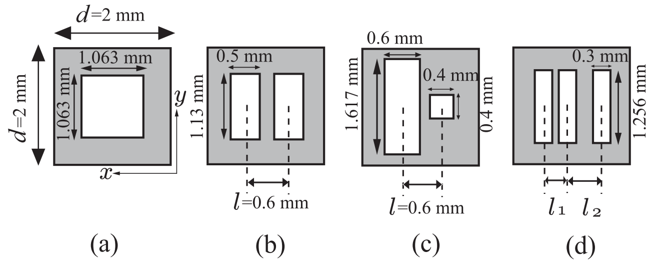

Figure 1. Schematic illustrations of four compound periodic hole arrays perforated on brass plates with the thickness $h = 2$ mm, period $d = 2$ mm and other geometrical parameters labeled, where only a unit cell for each hole array is plotted.

fraction 0.282. The other different parameters are the numbers and sizes of holes in a unit cell. In figures 1(b)–(d), a unit cell consists of two identical holes with size 0.5 mm × 1.13 mm and separation $l = 0.6$ mm, two different holes with sizes 0.6 mm × 1.617 mm and 0.4 mm × 0.4 mm and separation $l = 0.6$ mm, three identical holes with size 0.3 mm × 1.256 mm and separations l_1, l_2, respectively.

The theoretical treatment for these compound hole arrays is based on the modal expansion in the whole space. For an incident plane acoustic wave with wavelength λ, in incidence region I and transmission region III, the pressure fields can be expressed in terms of plane waves, which read

$$p^{\mathrm{I}} = \mathrm{e}^{\mathrm{i}(\boldsymbol{k}_{\|}^{\mathbf{0}}\cdot\boldsymbol{r}+k_z^0 z)} + \sum_{\boldsymbol{k}_{\|}} r_{\boldsymbol{k}_{\|}} \mathrm{e}^{-\mathrm{i}k_z z}\mathrm{e}^{\mathrm{i}\boldsymbol{k}_{\|}\cdot\boldsymbol{r}} \quad (1)$$

and

$$p^{\mathrm{III}} = \sum_{\boldsymbol{k}_{\|}} t_{\boldsymbol{k}_{\|}} \mathrm{e}^{\mathrm{i}k_z(z-h)}\mathrm{e}^{\mathrm{i}\boldsymbol{k}_{\|}\cdot\boldsymbol{r}}, \quad (2)$$

where $\boldsymbol{k}_{\|} = \boldsymbol{k}_{\|}^{\mathbf{0}} + \boldsymbol{G}$ is the vector parallel to the surface with $\boldsymbol{G}$ being the reciprocal vector of the hole lattice, and $r_{\boldsymbol{k}_{\|}}$ and $t_{\boldsymbol{k}_{\|}}$ are the reflection and transmission amplitudes.

In region II, the pressure field can be expanded in terms of the waveguide eigenmodes in holes as

$$p^{\mathrm{II}} = \sum_{j=1}^{N}\sum_{\alpha_j,\beta_j} \cos[\alpha_j(x-x_j)]\cos[\beta_j(y-y_j)] \times [C_{\alpha_j\beta_j}\mathrm{e}^{\mathrm{i}q_{\alpha_j\beta_j}z} + D_{\alpha_j\beta_j}\mathrm{e}^{-\mathrm{i}q_{\alpha_j\beta_j}z}], \quad (3)$$

where the subscript j denotes the hole and N is the number of holes in a unit cell. $q_{\alpha_j\beta_j} = \sqrt{\boldsymbol{k}^2 - \alpha_j^2 - \beta_j^2}$ with $|\boldsymbol{k}| = 2\pi/\lambda$ is the propagation constant of the waveguide mode $|\alpha_j\beta_j\rangle$ in hole j, $C_{\alpha_j\beta_j}$ and $D_{\alpha_j\beta_j}$ are the wave amplitudes, and $x_j(y_j)$ prescribes the central position of hole j.

For each subwavelength hole, it is enough to consider only the first waveguide eigenmode. In some situations, the plate is treated as rigid [13–15] and placed in water. Then for the first eigenmode, we can take $\alpha_j, \beta_j = 0$. By using the continuity of the pressure field p and the velocity field $v_z = -(1/\mathrm{i}\rho_0\omega)\partial p/\partial z$ at the two surfaces, we can derive a matrix equation for the unknown reflection and transmission amplitudes, where ρ_0 is the density of water and $\omega = c(2\pi/\lambda)$ is the angular frequency of the incident plane wave with the acoustic velocity $c = 1490$ m s^{-1}.

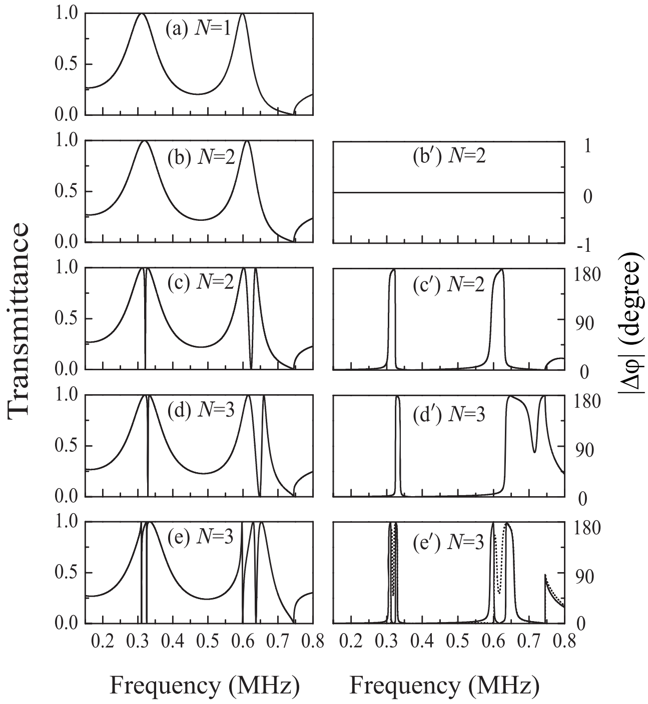

Figure 2. (a)–(e) Calculated transmittance for a normally incident acoustic wave impinging on the compound periodic hole arrays shown in figure 1. Here (d), (e) correspond to figure 1(d) with separations $l_1 = l_2 = 0.4$ mm and $l_1 = 0.4$ mm, $l_2 = 0.6$ mm, respectively. (b′)–(e′) Phase differences of the fields between adjacent holes for the structures considered in (b)–(e), respectively. N is the number of holes in a unit cell.

The left panels in figure 2 show the calculated transmittance spectra for the hole arrays shown in figure 1; among them, figures 2(a)–(c) correspond to figures 1(a)–(c) and figures 2(d) and (e) correspond to figure 1(d) with separations $l_1 = l_2 = 0.4$ mm and $l_1 = 0.4$ mm, $l_2 = 0.6$ mm, respectively. Comparing figure 2(a) here with figure 1(a) in the earlier work of Hou *et al* [13], we can observe that there is little difference between them. As was explained, the transmission peaks at the frequencies 0.310 and 0.598 MHz mainly arise from the FP resonances, and the minimum transmission at the frequency 0.745 MHz (corresponding to the wavelength 2 mm) results from the Wood anomaly. By calculating the transmission for different hole shapes (to keep the period and hole filling fraction invariant) we find that the hole shapes have little influence on EAT, which is different from the phenomenon for EOT [7]. In physics, it originates from the existence of zero-order waveguide mode for the acoustic case, which implies that the pressure field p^{II} is constant in the xy plane and independent of the hole shapes.

For the two-sublattice hole array with identical holes in a unit cell, it can be observed that the transmission spectrum shows little difference from figure 2(a) except that the FP resonance peaks are shifted slightly to higher frequencies, as shown in figure 2(b). However, it is found that each FP resonance peak splits into two parts for the two-sublattice hole array with two different holes in a unit cell, as shown in figure 2(c). In the case of three-sublattice hole arrays with identical holes, we also find that the FP resonance peaks split. More interesting is that each FP resonance peak splits into two when the separations between adjacent holes are equal, while it splits into three when they are unequal, as shown in figures 2(d) and (e), respectively. Since all the compound hole arrays have identical period, the transmission minimum from the Wood anomaly is always at the frequency 0.745 MHz, as shown in figures 2(b)–(e).

All the transmission spectra for the acoustic waves shown here have very similar features to the ones obtained through the compound metallic gratings in the electromagnetic case [16–18, 20]. So, like for the electromagnetic case, we calculate the phase difference of pressure fields between adjacent holes in a unit cell for the cases in figures 2(b)–(e), respectively. The calculated results are shown in figures 2(b′)–(e′). Comparing figures 2(b)–(e) with figures 2(b′)–(e′) respectively, we can find that each transmission dip, leading to the splitting of a FP resonance peak, has an exact correspondence to the π phase difference between adjacent holes. So we can conclude that the transmission dips arise from the field–phase interference between holes in a unit cell and so these can be called phase resonances.

The physical origins of phase resonances can be explained as follows. On one hand, it is well known that for a single periodic hole array, the translation invariance can reduce the field degrees of freedom to just a unit cell. Therefore, the fields in all holes are equal when a plane wave is normally incident. As for compound periodic hole arrays, this translation invariance can also reduce the degrees of freedom to a unit cell, but it cannot ensure that the fields of different holes in a unit cell are identical. On the other hand, the FP resonances arise from individual hole cavities, so the addition of extra hole cavities to each unit cell can introduce new FP modes (new degrees of freedom). These FP modes induced by different holes in a unit cell are degenerate if the holes have identical hole area, and nondegenerate if these hole areas are different. For the nondegenerate case, it is understandable that the field phases in different holes are unequal. Like for the electromagnetic case [16], when the phase difference between holes approaches π, the interference between them can lead to the appearance of transmission dips, as shown in figures 2(c) and (c′). As for the holes with same areas, it will be attested that the coupling between holes can remove the degeneracy of the FP modes. In fact, for the case in figure 2(c), the coupling between holes in a unit cell can also be of great importance. It is noted that holes can couple acoustically through diffraction modes, but the coupled FP modes strongly hybridize with ASWs, which are built up from periodic hole arrays [10, 21], instead of the diffraction evanescent waves [22]. The hybridized features can be understood analogously from the continuous evolution of dispersion curves from horizontal surface resonances (surface plasmon resonance) to vertical surface resonances (FP resonances) for deeper gratings in the electromagnetic case [23].

For a normally incident acoustic wave impinging at the compound periodic hole arrays with identical holes, the intensity of coupling between holes is only determined by the separations between them. In consequence, the possible phase configurations must be symmetrical when the arrangements of the holes in a unit cell are regular [16], such as the equal separations between adjacent holes. Accordingly, the degeneracy of the FP modes cannot be removed completely. Therefore, for the hole arrays in figure 1(b), the field phases in the two holes are equal due to the symmetry, as found in figure 2 (b′). Similarly, for the three-sublattice hole array with identical holes, the field phases in the external two holes must be identical when the separations between adjacent holes are equal, yet the field phases in the central hole and the external holes are different, as shown in figure 2(d′). The null phase difference between the external two holes implies that the degeneracy of the FP modes induced by the two holes cannot be removed. As a result, there is only one transmission dip appearing in each FP resonance peak in this three-sublattice hole array, as shown in figure 2(d). When the separations between adjacent holes in a unit cell are unequal, the symmetry is broken entirely and then the degeneracy of the FP modes is removed completely. It can be observed that each FP peak splits into three peaks with two phase resonance dips, as found in figures 2(e) and (e′). In addition, we observe that there is a π phase difference at frequency around 0.745 MHz in figure 2(d′), but it does not correspond to a transmission dip in figure 2(d). This is because of the complex interplay between the FP modes and surface modes, where the plate thickness plays a central role. The transmission peaks and dip around 0.745 MHz just do not display at the thickness $h = 2$ mm, but the related π phase difference has existed. We can find that this π phase difference does correspond to a transmission dip when we slightly increase the plate thickness.

Non-normal incidence is a more complex situation. The intensity of the coupling between holes will be affected by the incidence angle. The possible phase configurations cannot remain symmetrical even though the holes are symmetrically arranged in a unit cell, which has been shown similarly in the electromagnetic case [17, 20]. Therefore, we can expect to remove all the degeneracy of the FP modes by taking a plane wave impinging at the compound arrays in figures 1(b) and (d) non-normally. Figure 3 shows the grayscale plots of transmittance as a function of the incidence angle and frequency. For convenience, the angle-dependent transmission through the single periodic hole array in figure 1(a) is also given in figure 3(a), from which we observe that there are two FP resonance bands (lighter zones). One band at a frequency around 0.3 MHz is hardly affected by the incidence angle, whereas the other band at a frequency that is $\in [0.5, 0.6]$ MHz is angle dependent, which indicates that this FP mode strongly hybridizes with the acoustic surface modes. In figure 3(b), which corresponds to the hole array in figure 1(b), we can find that a phase resonance band (gray zone) appears within each FP resonance band when the incidence angle changes. The appearance of the phase resonance bands manifests that the field phases in the two holes are no longer equal and the degeneracy of the FP modes has been broken in the oblique incidence case, which can be demonstrated by its phase difference curve (not shown). Similarly, for the hole array in figure 1(d) with separations $l_1 = l_2 = 0.4$ mm, we can observe that there are two phase resonance bands within each

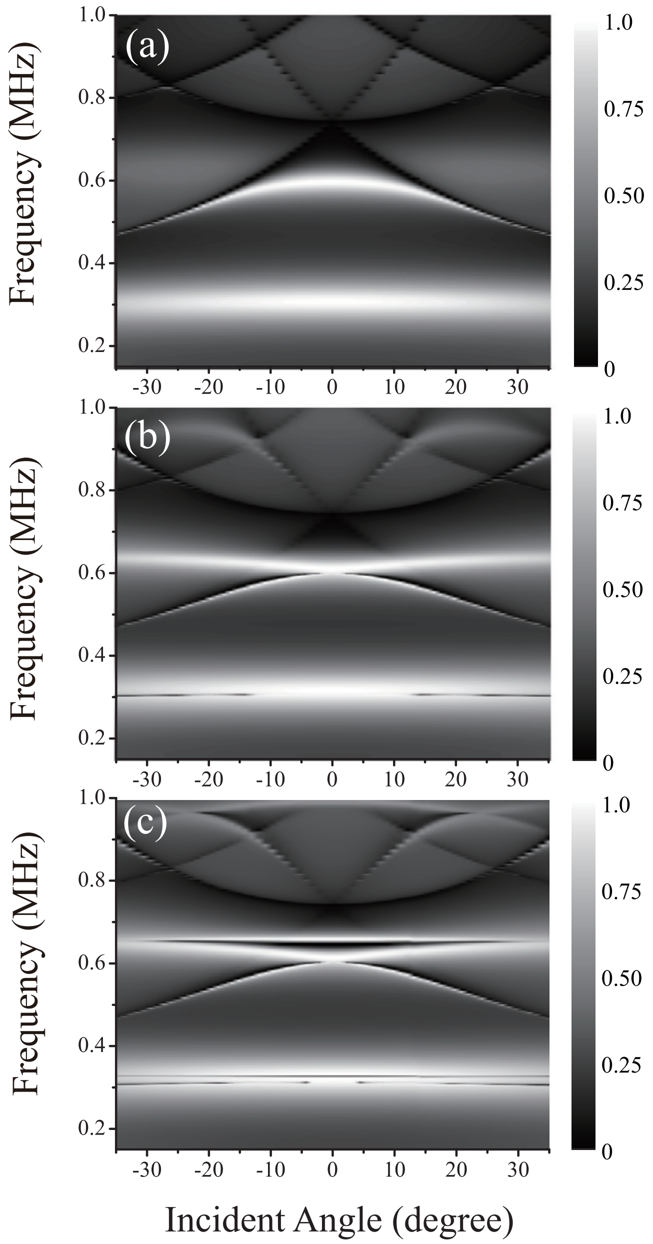

Figure 3. Grayscale plots of transmittance, as a function of incidence angle and frequency, through the hole arrays considered in figures 1(a), (b) and (d) with separations $l_1 = l_2 = 0.4$ mm, respectively.

FP resonance band under non-normal incidence, as shown in figure 3(c). For frequency that is $\in$ [0.5, 0.6] MHz, we can observe that the phase resonance band is angle dependent and adheres to the transmission band, as found in figures 3(b) and (c), respectively. This characteristic indicates that not only the FP resonances but also the relevant phase resonances can be greatly affected by ASWs. In figures 3(b) and (c) at a frequency around 0.62 MHz, another angle-independent FP resonance band appears, which further demonstrates that the addition of holes per period can introduce new FP modes (new degrees of freedom). The coupling of these degenerate FP modes induces the breaking of the degeneracy and then leads to the appearance of phase resonances.

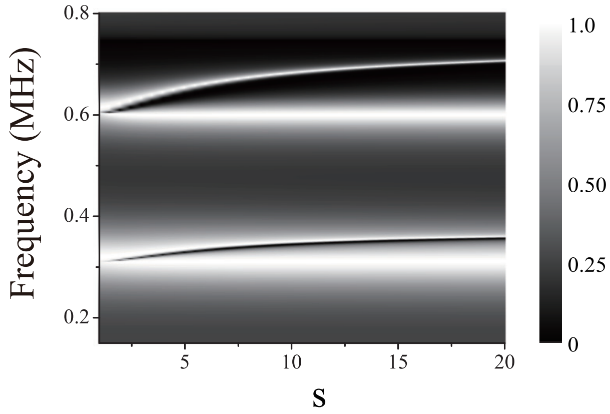

Figure 4. Grayscale plot of transmittance as a function of hole area ratio S and frequency for a normally incident plane wave impinging on two-sublattice periodic hole arrays perforated on the plates with the thickness 2 mm. The period 2 mm, separation between holes 0.6 mm and hole filling fraction 0.282 remain invariant.

For the two-sublattice hole array in figure 1(c), we cannot get any new phase resonance dips by changing the incidence angle because the degenerate FP modes have been opened up. However, due to the fact that the difference of the hole areas plays a leading role in the appearance of phase resonances, it can be expected to tune the phase resonance dip at the normal incidence by adjusting the hole area ratio S between the two holes in a unit cell (to keep the hole filling fraction constant). There are some features in common with the adjusting of the slit length in the compound metallic slits [19]. In essence, it is the modulation of the coupling between holes. The calculated grayscale plot of transmittance versus frequency and hole area ratio S is shown in figure 4, from which we can find that the widening of the phase resonance dip at a frequency around 0.6 MHz is proportional to the area ratio S, but it has little dependence on the area ratio at a frequency around 0.3 MHz. From the preceding discussion, we see that the FP mode at a frequency around 0.6 MHz strongly hybridizes with the acoustic surface modes, so the relevant phase resonance band must be sensitive to the array period and area fraction of holes. However, the other resonance band at a frequency around 0.3 MHz is hardly affected by the ASWs; thus the relevant phase resonance is insensitive to the hole area ratio of holes. It is noted that there is no dip found when the area ratio equals 1, just as in figure 2(a). By adjusting the area ratio between holes, we can achieve a wide range of acoustic screening at frequency lower than that of the Wood anomaly [24].

Other than the FP resonances and the phase resonances discussed above, for a perfect rigid plate with a periodic hole array, acoustic surface modes are built up and they can lead to transmission resonance at wavelength $\lambda \approx d$. Due to the comparability of the acoustic transmission through subwavelength apertures and the optical transmission through metallic gratings, we can get band structures similar to those presented with the metallic gratings [9, 23] to distinguish the transmission resonances involving the surface modes and FP resonance in the acoustic case. As was explained for the metallic gratings, the resonance peaks arising from the surface plasmon resonances can be affected by the grating thickness [9] and the surface plasmon resonances can continuously evolve into FP resonances for greater thickness [23]. This is also the case for the acoustic transmission. The calculations can manifest that, for the hole arrays with thickness $h = 0.1$ mm, a remarkable resonance peak appears at wavelength slightly larger than the array period and this resonance peak does not split even for compound hole arrays. Both features tell us that this resonance peak originates from the acoustic surface mode, completely. However, on increasing the plate thickness, we can observe that a series of peaks at wavelength $\lambda > d$ emerges and the splitting of these peaks can be found for compound hole arrays. In addition, the continuous transitions between the acoustic surface modes and FP modes can also be obtained for deeper hole arrays. All of these characteristics imply hybridization between the surface modes and FP modes in the resonant acoustic transmission.

In conclusion, we have studied the resonant acoustic transmission through several kinds of compound periodic hole arrays with acoustic waves at normal and non-normal incidence. A new resonance mechanism, phase resonances, is found. The phase resonances, arising from the coupling between holes in a unit cell, are characterized by the π phase difference between adjacent holes and exhibited as sharp dips in transmittance spectra. Moreover, the transmission resonance stemming from the ASWs is also discussed briefly and the hybridized features, of the surface modes and FP modes, are further demonstrated. Our results may be useful for tailoring the acoustic transmission properties and are expected to have applications in soundproofing engineering and acoustic filters.

Acknowledgments

This work was supported by the National Natural Science Foundation of China (Grant Nos 10674058, 60876065) and the State Key Program for Basic Research of China (Grant Nos 2006CB921803, 2009CB929504).

References

[1] Ebbesen T W, Lezec H J, Ghaemi H F, Thio T and Wolff P A 1998 *Nature* **391** 667
[2] Ghaemi H F, Thio T, Grupp D E, Ebbesen T W and Lezec H J 1998 *Phys. Rev.* B **58** 6779
[3] Martín-Moreno L, García-Vidal F J, Lezec H J, Pellerin K M, Thio T, Pendry J B and Ebbesen T W 2001 *Phys. Rev. Lett.* **86** 1114
[4] Barnes W L, Dereux A and Ebbesen T W 2003 *Nature* **424** 824
[5] Pendry J B, Martín-Moreno L and Garcia-Vidal F J 2004 *Science* **305** 847
[6] Liu H and Lalanne P 2008 *Nature* **452** 728
[7] van der Molen K L, Koerkamp K J K, Enoch S, Segerink F B, van Hulst N F and Kuipers L 2005 *Phys. Rev.* B **72** 045421
[8] Ruan Z and Qiu M 2006 *Phys. Rev. Lett.* **96** 233901
[9] Porto J A, Garcia-Vidal F J and Pendry J B 1999 *Phys. Rev. Lett.* **83** 2845
[10] Christensen J, Fernandez-Dominguez A I, de Leon-Perez F, Martin-Moreno L and Garcia-Vidal F J 2007 *Nat. Phys.* **3** 851
[11] Zhang X 2005 *Phys. Rev.* B **71** 241102
[12] Lu M H, Liu X K, Feng L, Li J, Huang C P, Chen Y F, Zhu Y Y, Zhu S N and Ming N B 2007 *Phys. Rev. Lett.* **99** 174301
[13] Hou B, Mei J, Ke M, Wen W, Liu Z, Shi J and Sheng P 2007 *Phys. Rev.* B **76** 054303
[14] Christensen J, Martin-Moreno L and Garcia-Vidal F J 2008 *Phys. Rev. Lett.* **101** 014301
[15] Estrada H, Candelas P, Uris A, Belmar F, Meseguer F and García de Abajo F J 2008 *Appl. Phys. Lett.* **93** 011907
[16] Skigin D C and Depine R A 2005 *Phys. Rev. Lett.* **95** 217402
[17] Ma Y G, Rao X S, Zhang G F and Ong C K 2007 *Phys. Rev.* B **76** 085413
[18] Navarro-Cía M, Skigin D C, Beruete M and Sorolla M 2009 *Appl. Phys. Lett.* **94** 091107
[19] Skigin D C, Loui H, Popovic Z and Kuester E F 2007 *Phys. Rev.* E **76** 016604
[20] Skigin D C and Depine R A 2006 *Phys. Rev.* E **74** 046606
[21] Kelders L, Allard J F and Lauriks W 1998 *J. Acoust. Soc. Am.* **103** 2730
Kelders L, Lauriks W and Allard J F 1998 *J. Acoust. Soc. Am.* **104** 882
[22] García-Vídal F J, Rodrigo S G and Martín-Moreno L 2006 *Nat. Phys.* **2** 790
[23] Collin S, Pardo F, Teissier R and Pelouard J L 2002 *J. Opt. A: Pure Appl. Opt.* **4** S154–60
[24] Estrada H, Candelas P, Uris A, Belmar F, García de Abajo F J and Meseguer F 2008 *Phys. Rev. Lett.* **101** 084302